STEM CELLS
TRANSLATIONAL MEDICINE®

TISSUE-SPECIFIC PROGENITOR AND STEM CELLS

Institutes of [a]Clinical Medicine, [h]Pharmacology, and [i]Traditional Medicine, School of Medicine, National Yang-Ming University, Taipei, Taiwan, Republic of China; [j]Stem Cell Laboratory, Department of Medical Research and [k]Orthopaedics and Traumatology, Taipei Veterans General Hospital, Taipei, Taiwan, Republic of China; [l]Institute of Biomedical Sciences, Academia Sinica, Taipei, Taiwan, Republic of China; [e]Graduate Institute of Clinical Medical Science, China Medical University, Taichung, Taiwan, Republic of China; [f]Department of Medical Research, China Medical University Hospital, Taichung, Taiwan, Republic of China; [g]Department of Health and Nutrition Biotechnology, Asia University, Taichung, Taiwan, Republic of China; [c]Institute of Cellular and System Medicine, National Health Research Institutes, Zhunan, Miaoli, Taiwan, Republic of China; [b]Department of Medicine, Feng-Yuan Hospital, Ministry of Health and Welfare, Executive Yuan, Taichung, Taiwan, Republic of China; [d]Taiwan Bio Therapeutics, Taipei, Taiwan, Republic of China

Correspondence: Shih-Chieh Hung, M.D, Ph.D., Department of Medical Research, Taipei Veterans General Hospital, 201, Section 2, Shih-Pai Road, Taipei 11217, Taiwan, Republic of China. Telephone: 886-2-77368497; E-Mail: hungsc@vghtpe.gov.tw; or Guei-Jane Wang, Ph.D., Graduate Institute of Clinical Medical Science, China Medical University, Taichung 40402, Taiwan, Republic of China. Telephone: 886-4-22337440; E-Mail: jennyw355@gmail.com

Received April 24, 2014; accepted for publication October 15, 2014.

Mesenchymal Stem Cells Ameliorate Atherosclerotic Lesions via Restoring Endothelial Function

YU-LING LIN,[a,b] SHAW-FANG YET,[c] YUAN-TONG HSU,[d] GUEI-JANE WANG,[e,f,g] SHIH-CHIEH HUNG[a,h,i,j,k,l]

Key Words. Mesenchymal stem cells (MSCs) • Human umbilical vein endothelial cells • Oxidized LDL • Atherosclerosis • Endothelial nitric-oxide synthase • Interleukin-8 • MIP-2 • p38 MAPK pathway • Apolipoprotein E-deficient

ABSTRACT

Transplantation of mesenchymal stem cells (MSCs) is beneficial in myocardial infarction and hind limb ischemia, but its ability to ameliorate atherosclerosis remains unknown. Here, the effects of MSCs on inhibiting endothelial dysfunction and atherosclerosis were investigated in human/mouse endothelial cells treated with oxidized low-density lipoprotein (oxLDL) and in apolipoprotein E-deficient (apoE$^{-/-}$) mice fed a high-fat diet. Treatment with oxLDL inactivated the Akt/endothelial nitric-oxide synthase (eNOS) pathway, induced eNOS degradation, and inhibited nitric oxide (NO) production in endothelial cells. Coculture with human MSCs reversed the effects of oxLDL on endothelial cells and restored Akt/eNOS activity, eNOS level, and NO production. Reduction of endothelium-dependent relaxation and subsequent plaque formation were developed in apoE$^{-/-}$ mice fed a high-fat diet. Systemic infusion with mouse MSCs ameliorated endothelial dysfunction and plaque formation in high-fat diet-fed apoE$^{-/-}$ mice. Interestingly, treatment with interleukin-8 (IL8)/macrophage inflammatory protein-2 (MIP-2) alone induced the similar effects of human/mouse MSCs on oxLDL-treated human/mouse endothelial cells. Neutralization antibodies (Abs) against IL8/MIP-2 also blocked the effects of human/mouse MSCs on oxLDL-treated human/mouse endothelial cells. Consistently, MIP-2 injection alone induced the similar effect of MSCs on the endothelial function in high-fat diet-fed apoE$^{-/-}$ mice. The improvement in endothelial dysfunction by mouse MSCs was also blocked when pretreating MSCs with anti-MIP-2 Abs. In conclusion, MSC transplantation improved endothelial function and plaque formation in high-fat diet-fed apoE$^{-/-}$ mice. Activation of the Akt/eNOS pathway in endothelium by IL8/MIP-2 is involved in the protective effect of MSCs. The study helps support the use and clarify the mechanism of MSCs for ameliorating atherosclerosis. STEM CELLS TRANSLATIONAL MEDICINE 2015;4:1–12

INTRODUCTION

Atherosclerosis, a vascular disorder leading to alterations and lesions in the inner walls of the blood vessels, underlies several important complications, such as coronary artery disease, stroke, and peripheral arterial disease [1]. Although its etiology is multifactorial, hypercholesterolemia plays a dominant role. It is generally thought that modifications of low-density lipoprotein (LDL) lead to its recognition and uptake by macrophage scavenger receptors, resulting in cholesteryl ester accumulation. Modified forms of LDL, such as oxidized LDL (oxLDL), have been previously linked to atherosclerosis [2]. oxLDL promotes endothelial dysfunction by exerting direct cytotoxicity on endothelial cells [3] and also by enhancing the production of inflammatory mediators [4]. Moreover, oxLDL inhibits endothelial nitric-oxide synthase (eNOS) activity and nitrogen oxide (NO) production, leading to interruption of NO-mediated responses in endothelial cells [5], which is partly attributed to the

downregulation of cellular eNOS via the ubiquitin-proteasome pathway (UPP) [6].

NO plays an important role in maintaining vessel functions, including vascular tone, platelet aggregation, smooth muscular proliferation, and leukocyte adhesion to endothelial cells [7]. The preponderant isoform of NOS in healthy endothelial cells is eNOS. The endothelium-dependent vasorelaxation is eNOS-dependent because eNOS$^{-/-}$ mice show elevated systemic and pulmonary arterial pressures and reduced endothelium-dependent relaxations in response to acetylcholine [8]. For well-controlled normal NO production, eNOS activity is highly regulated by post-translational modifications. Phosphorylation of eNOS at Ser1177 by Akt/protein kinase B activates eNOS [9], whereas disruption of its association with Akt by oxLDL deactivates eNOS [10]. Besides, eNOS availability regulated by the UPP also plays a crucial role in maintaining vessel functions [11], despite few studies in this area.

Bone marrow-derived mesenchymal stem cells (MSCs) are capable of self-renewal and have

the potential to differentiate into mesenchymal and nonmesenchymal tissues [12]. They target injuries of the heart [13] and engraft for regeneration. MSCs, when transplanted in a murine model of hind limb ischemia, revascularize and ameliorate the ischemic limb [14]. Moreover, transplantation of MSCs rejuvenated by the overexpression of telomerase and myocardin promotes revascularization and tissue repair in ischemic limb [15]. The effect of MSC therapy has recently been reported to be affected by a mechanism of endocrine or paracrine effects [16, 17]. Although transplantation of MSCs is beneficial in treating myocardial infarction and hind limb ischemia, its ability to ameliorate atherosclerosis remains unknown.

Because atherosclerosis is a chronic disease requiring lifetime preventive therapy, multiple steps in the atherogenic process could theoretically serve as the target for intervention. To further understand the therapeutic effects of MSCs on ameliorating atherosclerotic lesions, we first treated oxLDL-exposed endothelial cells with MSCs and examined the effects of MSCs on blocking oxLDL-induced changes. We then treated apolipoprotein E-deficient (apoE$^{-/-}$) mice that had been fed with high-fat diet for 5 weeks with MSCs and investigated the effects of MSCs on ameliorating atherosclerosis-induced changes including the early endothelial function and subsequent plaque burden. We further identified the key factor and the underlying mechanism that MSCs mediated to provide the therapeutic effects on ameliorating atherosclerosis-induced changes.

MATERIALS AND METHODS

Reagents

LDL was purchased from Merck (Darmstadt, Germany, http://www.merck.com). Endothelial cell growth medium-2 (ECGM-2) was purchased from PromoCell (Heidelberg, Germany, http://www.promocell.com). Antibodies (Ab) against Akt, phospho-Akt (Ser473), eNOS, and phospho-eNOS (Ser1177), phospho-p38, p38, extracellular regulated protein kinases (ERK), phospho-ERK, c-Jun N-terminal kinases (JNK), and phospho-JNK were obtained from Cell Signaling Technology (Beverly, MA, http://www.cellsignal.com).

oxLDL Preparation

Plasma in the presence of EDTA was used to isolate LDL by sequential ultracentrifugation ($1.019 < d < 1.063$ kg/l). Afterward, native LDL was dialyzed at 4°C for 24 hours against 1,000 volumes of phosphate-buffered saline (PBS) to remove EDTA. To initiate oxidation, LDL (0.5 g of protein per liter) was exposed to 5 μM $CuSO_4$ for 18 hours. The generation of thiobarbituric acid-reactive substances was monitored by the fluorometric method as described previously [18], and the values of the malondialdehyde equivalents increased from 0.76 ± 0.21 nmol/mg protein of native LDL to 24.3 ± 2.6 nmol/mg protein of $CuSO_4$-treated LDL. The freshly prepared oxLDL was dialyzed at 4°C for 48 hours against 500 volumes of PBS to remove Cu^{2+} and was sterilized by passage through a 0.22-μm filter. The protein contents of native LDL and the oxLDL preparations were measured by the Lowry assay [19].

Cells and Culture Conditions

Primary human MSCs (hMSCs) were obtained using the protocol as described previously [20]. Briefly, bone marrow aspirates were taken from the iliac crest of normal adult donors after informed consent and under a protocol approved by an institutional review board. Nucleated cells were isolated by a density gradient (Ficoll-Paque; Pharmacia, Peapack, NJ, http://www.pfizer.com) and resuspended in complete culture medium (α-minimal essential medium [α-MEM]; Gibco-BRL, Gaithersburg, MD, http://www.invitrogen.com) supplemented with 10.0% fetal bovine serum (FBS), 100 units/ml penicillin, 100 μg/ml streptomycin, and 2 mM L-glutamine. Human umbilical vein endothelial cells (HUVECs) were obtained from the Bioresource Collection and Research Center (Hsinchu, Taiwan), cultured in ECGM-2 according to the manufacturer's instructions, and used in passages 6–8. Cells were maintained at 37°C under 5% CO_2. Mouse MSCs (mMSCs) were obtained from 4–6-week-old C57BL/6 mice and cultured in α-MEM supplemented with 10% FBS as previously described [21]. In brief, the bone marrow collected from the femurs and tibiae of five inbred C57BL/6 mice was used to isolate mMSCs. The mononuclear cells harvested from bone marrow were plated in 10-cm dishes under hypoxic (1% O_2) conditions. For maintenance of the hypoxic gas mixture, an incubator with two air sensors, one for CO_2 and the other for O_2, was used; the O_2 concentration was achieved and maintained using delivery of nitrogen gas (N_2) generated from a tank containing pure N_2. If the O_2 percentage rose above the desired level, N_2 gas was automatically injected into the system to displace the excess O_2. After 24 hours, nonadherent cells were removed by washing with phosphate-buffered saline (PBS) and 10 ml of fresh growth medium was added. mMSCs were characterized to be positive for Sca-1, CD29, CD44, and CD105 but negative for CD11b, CD31, CD34, and CD45. Moreover, mMSCs possess the ability to differentiate into osteoblasts, adipocytes, and chondrocytes [21]. The mMSCs were used at passage 3. Mouse brain microvascular endothelial cells (MMECs) were isolated from 4–6-week-old C57BL/6 mice as previously described [22]. The cells were then cultured in high-glucose Dulbecco's modified Eagle's medium (HG-DMEM) + 10% FBS.

Western Blot Analysis

Cell extracts were prepared with Mammalian Protein Extraction Reagent (M-PER) (Pierce, Rockford, IL, http://www.piercenet.com) plus protease inhibitor cocktail (Halt; Pierce), and protein concentrations were determined using the bicinchoninic acid assay (Pierce). Equal amounts of cellular proteins were then electrophoresed in an SDS-polyacrylamide gel, and proteins were then transferred to polyvinylidene difluoride membranes (Amersham Biosciences, Piscataway, NJ, http://www.amersham.com). Nonspecific binding sites on the membranes were blocked with 5% nonfat milk at 4°C overnight. Membranes were reacted with first Ab. The membranes were then probed with their respective secondary Ab conjugated with horseradish peroxidase. The bands were visualized using an enhanced chemiluminescence kit (PerkinElmer Life and Analytical Sciences, Waltham, MA, http://www.perkinelmer.com) and detected with x-ray film.

Transwell Migration Assay

Equal aliquots of HUVECs (5×10^5) in 600 μl of ECGM-2 + 10% FBS without or with oxLDL (50 μg/ml) were placed in the low chambers of Costar polycarbonate Transwells (8-μm pore size; Corning Costar, Acton, MA, http://www.corning.com/lifesciences), whereas 1×10^5 MSCs in 100 μl of ECGM-2 + 1% FBS were added to the top chambers of the Transwells. Cells without oxLDL treatment served as the control. After migration for 24 hours, the

remaining cells on the upper surface of the membrane were re-moved by wiping with a cotton swab, and migratory cells on the membrane underside were fixed using 5% (wt/vol) glutaral-dehyde and stained using 4′,6-diamidino-2-phenylindole (DAPI). The filter inserts were inverted, and the numbers of DAPI-stained cells were determined by fluorescence microscopy. The data are presented as the average number of migratory cells calculated from 8 high-power fields ($\times$200). Each experiment was per-formed in triplicate, and then the data were averaged for statis-tical analysis. For neutralization of the effects of stromal cell-derived factor 1 (SDF-1) and C-X-C chemokine receptor type 4 (CXCR4), migration assays were performed in the presence of antibodies against SDF-1 (MAB310; R&D Systems Inc., Minneap-olis, MN, http://www.rndsystems.com), CXCR4 (MAB170; R&D Systems Inc.), or isotype IgG.

Real-Time RT-PCR

The mRNA levels were quantified by real-time reverse transcription (RT)-polymerase chain reaction (PCR) array on the RT^2 Profiler PCR Array of Human Cytokines & Chemokines (SABiosciences, Frederick, MD, http://www.sabiosciences.com/) according to the manufacturer's instructions. Briefly, total RNA (2 μg) was reverse-transcribed into first-strand cDNA and used as a template to perform real-time PCR on the ABI PRISM 7700 sequence detec-tion system (Applied Biosystems, Foster City, CA, http://www.appliedbiosystems.com). The PCR annealing step was at 60°C for 30 seconds. PCR amplification of glyceraldehyde-3-phosphate de-hydrogenase and hypoxanthine guanine phosphoribosyl transfer-ase 1 was performed for each sample to control for sample loading and allow for normalization between samples. The data were analyzed using the comparative $\Delta\Delta$Ct method, according to the PCR Array Data Analysis downloaded from the SABiosciences website. Expression of the target gene SDF-1α, interleukin-8 (IL8), macrophage inflammatory protein-2 (MIP-2) and the endogenous reference glyceraldehyde-3-phosphate dehydrogenase was quan-tified using the primers, probes, and standards. The primers and TaqMan probes were designed using the software Primer Express (Applied Biosystems). RT-PCR was performed according to a TaqMan two-step method using an ABI PRISM 7700 sequence de-tection system (Applied Biosystems).

Assay for NO Synthesis

NO levels were measured by the Griess method after conversion of nitrate to nitrite by nitrate reductase by using the commercially available kit (nitrate/nitrite colorimetric assay kit; Cayman Chem-icals, Ann Arbor, MI, http://www.caymanchem.com, catalog no. 780001) according to the manufacturer's recommendations. Briefly, 100 μl of culture supernatant was reacted with an equal volume of Griess reagent for 10 minutes at room temperature in the dark. Total nitrite was measured as NO levels at 540-nm ab-sorbance by reaction with Griess reagent (sulfanilamide and naphthalene-ethylene diamine dihydrochloride).

Animals and MSC Transplantation Regimen

The animal study protocol was approved by the Animal Experi-mental Committee of Taipei Veterans General Hospital. Male 8-week-old apolipoprotein E-deficient (apoE$^{-/-}$) mice (C57BL/6-KO-apoe^{tm1Unc}/J; Jackson Laboratories) were used for this study. The animals were maintained in a 22°C room with a 12-hour light/dark cycle and received drinking water ad libitum.

The 58Y1 diet (60% fat and 0.03% cholesterol; Test Diet, PMI Nu-trition International, Richmond, IN, http://www.testdiet.com) was chosen to create the atherosclerotic lesions because it ele-vates blood cholesterol levels similar to that in human atheroscle-rosis. All experimental mice were fed with 58Y1 for 5 weeks and then received a single dose of MSCs (2 $\times$ 10^5 cells) by intravenous tail vein injection. Control animals received a corresponding amount of PBS solution without cells. To evaluate the role of MIP-2 in the paracrine effect of MSCs, we used hMSCs pretreated with either MIP-2 Ab (clone 40605, IgG2bg; R&D Systems) or con-trol isotype IgG (clone 141945, IgG2b; R&D Systems). Moreover, at the end of the 5-week treatment period with high-fat diet, apoE$^{-/-}$ mice also received a single dose of MIP-2 (50 μg/kg) with-out cells by intraperitoneal injection. After cell/PBS, MIP-2 Ab/IgG, MIP-2 treatment, all mice were fed with normal chow for 7 days, when tissue samples and blood were collected immediately. Plasma lipid concentrations were determined by routine chemical methods.

Aortic Ring Preparations and Tension Recording

Sections of the thoracic aorta 2 mm below the subclavian artery were excised carefully and fixed isometrically in organ chambers (7 ml) containing a modified Krebs solution: 120 mM NaCl, 4.5 mM KCl, 2.5 mM CaCl$_2$, 1 mM MgSO$_4$, 27 mM NaHCO$_3$, 1 mM KH$_2$PO$_4$, and 10 mM glucose maintained at 37°C and through which a mix-ture of 95% O$_2$, 5% CO$_2$ was bubbled. The details of the prepara-tion procedure were described previously [23]. Briefly, aortic rings of 2 mm in length were equilibrated under passive tension for 30 minutes. During this time, the tissues were washed every 15 minutes. After equilibration, the aortic rings were stabilized with a near-maximal contraction induced by phenylephrine (10^{-6} M). After the rings achieved a stable contractile tension, drugs were added in increasing concentrations to obtain cumulative concentration-response curves: 10^{-9} to 10^{-5} M phenylephrine, 10^{-9} to 10^{-5} M acetylcholine (assessment of endothelium-dependent aortic ring relaxation after precontraction with phen-ylephrine), and 10^{-11} to 10^{-5} M nitroglycerin (assessment of endothelium-independent aortic ring relaxation after precontrac-tion with phenylephrine). The drug concentration was increased when aortic ring constriction or relaxation was completed. Drugs were washed out before the next substance was added.

Quantification of Aortic Atherosclerotic Lesions

For the quantification of atherosclerotic lesions of apoE$^{-/-}$ mice [17], serial sections were cut through the aorta at the origins of the aortic valve leaflets, and 40 serial sections from the aortic si-nus of each mouse were collected. For endothelial integrity, the aorta was not perfused with normal saline to prevent perfusion-related endothelial injury. Every tenth section (5 μm) throughout the aortic sinus (200 μm) was hematoxylin/eosin-stained, and the photomicrograph was taken. The cross-sectional area of a given photomicrograph was analyzed using computer imaging graphic software (IPWin32). Mean lesion area was quantified from the av-erage of five digitally captured sections per mouse.

Immunohistochemistry Study

Mouse sections were deparaffinized in xylene and hydrated in water. Tissue sections were pretreated with 3% H$_2$O$_2$ for 10 minutes at room temperature to inactivate the endogenous per-oxidase. Sections were blocked in PBS containing 1% BSA and 1% goat serum at 37°C for 30 minutes. The sections were incubated

with the appropriate Ab overnight, followed by wash with PBS. Slides were then incubated with a secondary Ab (goat anti-rat; BD Pharmingen, San Diego, CA, http://www.bdbiosciences.com) for 30 minutes. After washing with PBS three times, color was developed with 0.1% 3,3'-diaminobenzidine. A negative control was performed by incubating the sections with secondary Ab only (omission of primary Ab). The sections were then counterstained with hematoxylin and examined by light microscopy. To focus on the signal changes of the endothelial cell, the phospho-Akt- and phospho-eNOS-positive cells were quantified in the endothelial layer from the sections and averaged.

Statistical Analysis

All statistical analyses were performed with the SPSS software, version 18.0 (SPSS, Inc., Chicago, IL, http://www-01.ibm.com/software/analytics/spss/). Overall comparison between two groups was performed with the Student's t test. Comparison between three or more groups was performed by analysis of variance with appropriate post hoc least significant difference testing between different groups. Quantitative data were presented as means $\pm$ SEM from at least three independent experiments. The criterion of significance was set as $p < .05$.

RESULTS

hMSCs Restore Akt/eNOS Activation and Stabilize eNOS in oxLDL-Treated Endothelial Cells

To examine the tissue repair potential of exogenous MSCs on atherosclerotic lesion, we first examined the recruitment of hMSCs by atherosclerotic endothelium. Transwell migration assay demonstrated oxLDL-treated HUVECs increased in the recruitment of hMSCs compared with HUVECs treated with the vehicle (Fig. 1A). We also revealed that SDF-1α, the chemokine attracting hMSCs [24], expressed by HUVECs was dose-dependently enhanced by oxLDL treatment with the peak at 50 μg/ml (Fig. 1B), which was the concentration of oxLDL used in the following experiments. Moreover, we have shown that the induction of hMSC migration by oxLDL-treated HUVECs in the lower wells was abrogated by neutralizing antibodies against SDF-1 or its receptor, CXCR4, suggesting that SDF-1-CXCR4 is responsible for the induction of MSCs migration by HUVECs with oxLDL treatment (Fig. 1A). We then examined whether indirect coculture of hMSCs protected HUVECs from oxLDL-induced damage. It is well known oxLDL induces endothelium damage through the suppression of phospho-Akt, phospho-eNOS, and total eNOS levels [5]. As expected, HUVECs treated with oxLDL decreased in the levels of phospho-Akt, phospho-eNOS, and total eNOS (Fig. 1C). Interestingly, we found indirect coculture with hMSCs abrogated oxLDL-induced decrease in the levels of phospho-Akt, phospho-eNOS, and total eNOS (Fig. 1C). Similarly, coculture with hMSCs significantly enhanced NO production in oxLDL-treated HUVECs (Fig. 1D). Together, these data suggest that oxLDL-induced HUVEC damage can specifically attract hMSCs, which protect HUVECs from oxLDL-induced loss in the levels of phospho-Akt, phospho-eNOS, total eNOS, and NO production.

mMSCs Restore Endothelium-Dependent Relaxation and Inhibit Plaque Formation in an Animal Model of Atherosclerosis

Because our data showed that hMSCs specifically migrated to and restored the Akt/eNOS activation of oxLDL-treated endothelial cells in vitro, we hypothesized that systemic application of exogenous MSCs may repair the atherosclerotic endothelium or ameliorate plaque formation in animal models of atherosclerosis. Before application to the animal study, we confirmed that mMSCs also restored the levels of Akt/eNOS phosphorylation and total eNOS that were suppressed by oxLDL in MMECs (Fig. 2A). We then investigated whether a single intravenous infusion of mMSCs (2×10^5 cells) from mice improved endothelial function in apoE$^{-/-}$ mice fed a high-fat diet for 5 weeks. At 7 days of mMSCs treatment, plasma lipid concentrations following high-fat diet feeding were not different between apoE$^{-/-}$ animals treated with PBS (supplemental online Table 1), suggesting that infusion of mMSCs does not have an effect on the control of plasma lipid concentrations. However, tension recording of aortic rings revealed that treatment with mMSCs significantly increased the value of acetylcholine-dependent relaxation, but not the values of sodium nitroprusside-dependent relaxation and phenylephrine-dependent contraction, as compared with treatment with PBS (Fig. 2B), suggesting that mMSCs improve endothelium-dependent vasodilatation but not vasodilation dependent on vascular smooth muscle cells or contraction. Moreover, we found that mMSCs decreased aortic plaque burden compared with PBS (Fig. 2C, 2D). Consistent with the in vitro findings, mMSCs also significantly increased the levels of Akt/eNOS phosphorylation in the aortic endothelium, compared with PBS (Fig. 2E). These data suggest that exogenous mMSCs provide endothelium repair and plaque prevention benefits in an animal model of atherosclerosis.

IL8 Is Required for hMSC-Mediated Restoration of Akt/eNOS Activation and eNOS Stabilization

Our data showed that indirect coculture of human hMSCs restored the levels of Akt/eNOS activation and total eNOS in oxLDL-treated HUVECs, suggesting that a paracrine effect was involved. When analyzing the cytokine and chemokine profiles of hMSCs using a human PCR array, we then identified IL8 as the only cytokine or chemokine that hMSCs increased in expression upon exposure to oxLDL in the presence of HUVECs (Fig. 3A). A second experiment with quantitative RT-PCR confirmed oxLDL alone, independent of the presence or absence of HUVECs, enhanced IL8 expression by hMSCs (Fig. 3B). Because the paracrine factors that cells secrete can be accumulated in the condition medium, we used the condition medium derived from oxLDL-treated hMSCs (CM-hMSC) for the study (Fig. 3C). The CM-hMSC reversed the inhibitory effect of oxLDL on the levels of Akt/eNOS phosphorylation and total eNOS in a dose-dependent manner. The beneficial effect of CM-hMSC was blocked by adding IL8 neutralization Abs at the same time (Fig. 3C). Moreover, replacement of CM-hMSC with IL8 also increased the levels of phosphorylated Akt and eNOS in oxLDL-treated endothelial cells (Fig. 3D). We further demonstrated the involvement of the phosphatidylinositol 3'-kinase (PI3K)/Akt pathway in indirect coculture of MSCs or IL8-mediated effect. The PI3K inhibitor LY294002 significantly blocked the beneficial effect of MSCs or IL8 on oxLDL-induced changes in Akt and eNOS phosphorylation (Fig. 3D).

In addition, we also examined whether indirect coculture of hMSCs or treatment with IL8 attenuated the eNOS protein degradation induced by oxLDL. Immunoprecipitation using anti-eNOS Ab following immunoblotting with anti-ubiquitin Ab discovered the ubiquitination of eNOS was markedly attenuated by hMSCs (Fig. 3E). The effect of attenuation of eNOS ubiquitination
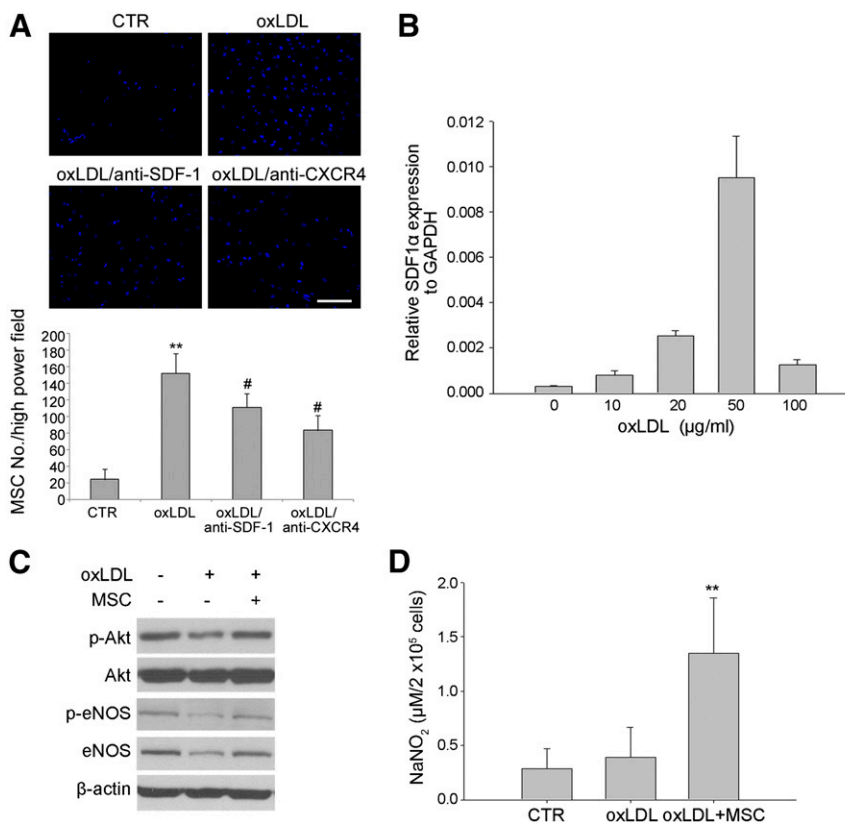
Figure 1. Effect of MSCs on oxLDL-induced human umbilical vein endothelial cell (HUVEC) damage. **(A):** Transwell migration assays. HUVECs were seeded in the lower wells without (CTR) or with oxLDL treatment (50 μg/ml) in the absence or presence of antibodies against SDF-1 (oxLDL/anti-SDF-1) or CXCR4 (oxLDL/anti-CXCR4), whereas MSCs were seeded in the upper wells and assayed at 24 hours. Top: Representative views of the fields in Transwell membranes, showing the stained MSCs that migrated to the lower membrane side of Transwells. Bottom: Quantification of the number of migrated MSCs per high power field. Data are the average numbers of migratory cells in eight high-power fields ($\times$200). Each experiment was performed in triplicate. $**$, $p < .01$ versus CTR; #, $p < .05$ versus oxLDL. **(B):** HUVECs were treated with the indicated concentrations of oxLDL for 24 hours, followed by quantitative reverse transcription-polymerase chain reaction analysis. **(C, D):** HUVECs (1.5×10^4 cells) were treated without or with 50 μg/ml oxLDL in the absence or presence of indirect coculture with MSCs (5×10^3 cells) for 24 hours, followed by Western blot analysis **(C)** and assay of the culture supernatants **(D)** for determining the NO production by using Griess method ($n = 6$ in each group). $**$, $p < .01$ versus CTR or oxLDL. Abbreviations: CTR, control; CXCR4, C-X-C chemokine receptor type 4; eNOS, endothelial nitric-oxide synthase; GAPDH, glyceraldehyde-3-phosphate dehydrogenase; MSC, mesenchymal stem cell; oxLDL, oxidized low-density lipoprotein; p-Akt, phospho-Akt; p-eNOS, phospho-eNOS; SDF-1, stromal cell-derived factor 1.

by hMSCs could be blocked by IL8 Ab (Fig. 3E). The effect of attenuation of eNOS ubiquitination was also observed in the presence of IL8 alone (Fig. 3E). Moreover, under the treatment of HUVECs with cycloheximide, which blocks protein synthesis, downregulation of eNOS expression after exposure to oxLDL was noted and improved after hMSCs treatment (Fig. 3F). Treatment with MG132, the proteasome inhibitor, abolished the downregulation of eNOS protein level, and the effect was similar to the hMSC treatment group. Besides, the upregulation of eNOS by hMSCs could be blocked by IL8 Ab. Moreover, IL8 treatment alone also upregulated eNOS level, and the effect was similar to the hMSC treatment group. These data suggest that besides the effect of the activation of phosphorylated eNOS, hMSCs also attenuate eNOS ubiquitination, and IL8 may play a key role in the paracrine effects of hMSCs.

MIP-2 Is Required for MSC-Mediated Restoration of Endothelium-Dependent Relaxation

We then elucidated the involvement of MIP-2, the IL8 homolog of mice, in mMSC-mediated beneficial effects in high-fat diet-fed apoE$^{-/-}$ mice. The pattern of MIP-2 expression as analyzed by quantitative RT-PCR in oxLDL-exposed mMSCs was similar to IL8 expression in oxLDL-exposed hMSCs (Fig. 4A). To further elucidate the role of MIP-2 in the paracrine effect of mMSCs in vivo, mMSCs were pretreated with anti-MIP-2 Ab or isotype IgG before injection into the high-fat diet-fed apoE$^{-/-}$ mice. The improvement in acetylcholine-dependent relaxation of aortic rings at 7 days after infusion with mMSCs was significantly blocked by pretreatment of mMSCs with anti-MIP-2 Ab but not with isotype IgG (Fig. 4B). A trend to abrogate the beneficial effect of mMSCs on aortic plaque burden was also observed after pretreatment of mMSCs with anti-MIP-2 Ab compared with isotype IgG, although a significant difference was not achieved (Fig. 4C). Moreover, the mMSC-mediated increases in the percentages of phospho-Akt+ and phospho-eNOS+ endothelial cells were significantly blocked by pretreatment of MSCs with anti-MIP-2 Ab compared with isotype IgG in vivo (Fig. 4D). Together, these data suggest that systemic application of exogenous mMSCs repairs the diseased endothelium and improves endothelial function via secretion of the IL8 homolog, MIP-2, by mMSCs.
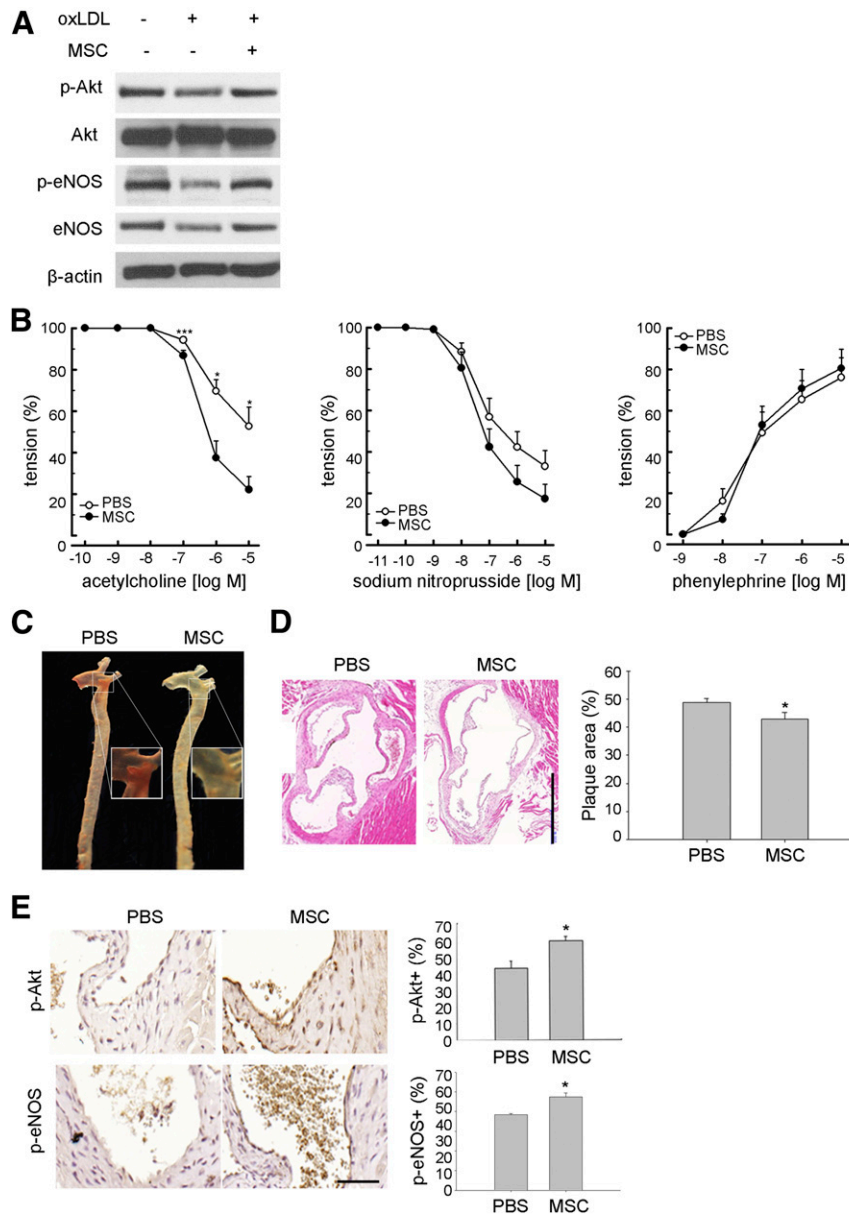
Figure 2. Effect of transplantation of mouse MSCs on high-fat diet-fed apoE$^{-/-}$ mice. **(A):** Mouse brain microvascular endothelial cells (1.5 × 10^4 cells) were treated without or with 50 μg/ml oxLDL in the absence or presence of indirect coculture with mouse MSCs (5 × 10^3 cells) in each well of a 24-well plate for 24 hours, followed by cell recovery for Western blot analysis. **(B–D):** High-fat diet-fed apoE$^{-/-}$ mice treated without (PBS, vehicle control) or with MSCs (2 × 10^5 cells) were sacrificed at 1 week after treatment. **(B):** The thoracic aortic rings were isolated freshly for determining the concentration-response curves of acetylcholine-dependent relaxation (left), sodium nitroprusside-dependent relaxation (middle), and phenylephrine-dependent contraction (right) (n = 5–6 in each group). ∗, $p < .05$; ∗∗, $p < .01$; ∗∗∗, $p < .001$ MSC versus vehicle control at the indicated concentrations. **(C):** The aortas subjected to plaque formation analysis by Oil Red O staining were longitudinally incised. Representative atherosclerotic lesions are red in color. **(D):** Representative aortic root microsections show the plaque formation (left). Right: Quantitative data are expressed as percentages of the total luminal surface area of the aorta (n = 3–4 in each group). ∗, $p < .05$. **(E):** Immunostaining of phospho-Akt and phospho-eNOS protein expression (left). Representative aortic root sections show phospho-Akt and phospho-eNOS expression in the endothelial lining. Right: Quantitative data are expressed as percentages of immunopositive cells of total endothelial lining cells (n = 3–4 in each group). ∗, $p < .05$. Scale bars = 500 μm **(D)**, 50 μm **(E)**. Magnification, ×40 **(C)**, ×400 **(D)**. Abbreviations: eNOS, endothelial nitric-oxide synthase; MSC, mesenchymal stem cell; oxLDL, oxidized low-density lipoprotein; p-Akt, phospho-Akt; PBS, phosphate-buffered saline; p-eNOS, phospho-eNOS.

MIP-2 Restores Endothelium-Dependent Relaxation

To demonstrate that MIP-2 is essential in mediating the effects of mMSCs in protecting endothelium from atherosclerosis-induced dysfunction and inhibiting plaque formation, we evaluated the direct effect of MIP-2 on restoring endothelial function and inhibiting plaque formation. Intraperitoneal injection of high-fat diet-fed apoE$^{-/-}$ mice with MIP-2 (50 μg/kg) significantly increased the acetylcholine-dependent relaxation of aortic rings at 7 days compared with vehicle alone (Fig. 5A). The therapeutic potential of MIP-2 on improving the endothelial function is obvious,
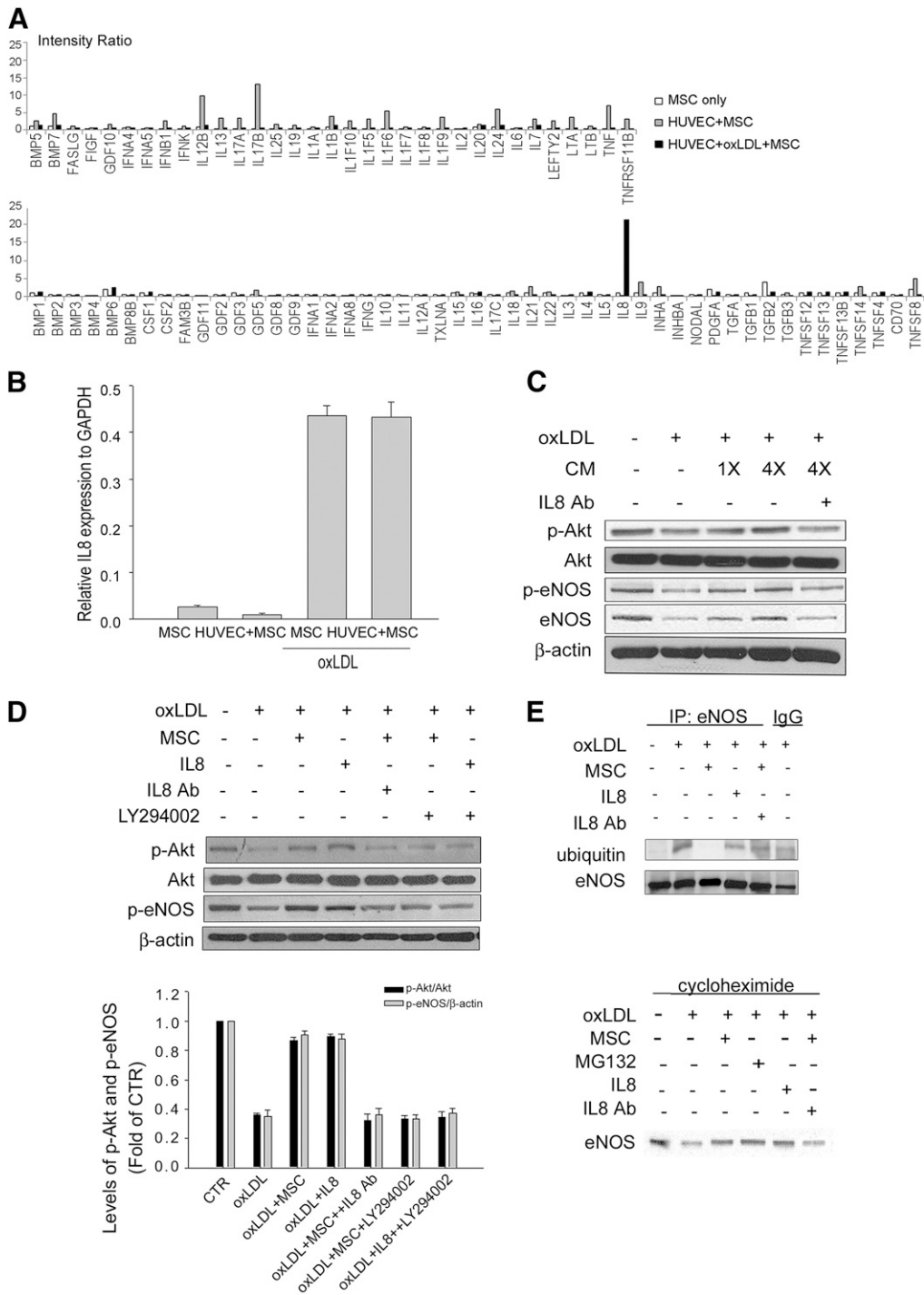
Figure 3. IL8 plays an important role in MSC-mediated effects on oxLDL-induced HUVEC damage. **(A, B):** Aliquots of MSCs (2×10^4 cells) alone or indirect coculture with HUVECs (6×10^4 cells) in the absence (HUVEC + MSC) or presence of 50 μg/ml oxLDL for 24 hours were assayed for quantitative reverse transcription (RT)-polymerase chain reaction (PCR). **(A):** The bar plot showing the relative mRNA levels as analyzed by the RT^2 Profiler PCR Array. The IL8 gene expression is increased in oxLDL + HUVEC + MSC compared with MSC alone or HUVEC + MSC. **(B):** Quantitative RT-PCR for IL8 mRNA levels. **(C):** Western blot analysis of HUVECs treated without or with 50 μg/ml oxLDL for 24 hours in the absence or presence of indicated folds of condition medium derived from oxLDL-treated MSCs (condition medium). **(D, E):** Western blot analysis **(D)** or immunoprecipitation with anti-eNOS Ab **(E)** followed by immunoblotting with anti-ubiquitin Ab of HUVECs treated without or with 50 μg/ml oxLDL for 24 hours in the absence or presence of MSCs, IL8, anti-IL8 Ab, or phosphatidylinositol 3′-kinase inhibitor LY294002. **(D):** The bottom panel shows the quantitative data obtained from the top panel. **(F):** Influence of MSC or IL8 on eNOS protein stability in the HUVECs. Under the treatment of HUVECs with cycloheximide, downregulation of eNOS level after exposure to oxLDL is improved after MSC treatment. Treatment with MG132 abolished the downregulation of eNOS level, and the effect is similar to the MSC treatment group (IL8: 10 ng/ml; IL8 Ab: 1,500 ng/ml; LY294002: 20 μM). Abbreviations: Ab, antibody; CTR, control; eNOS, endothelial nitric-oxide synthase; GAPDH, glyceraldehyde-3-phosphate dehydrogenase; HUVEC, human umbilical vein endothelial cell; IL8, interleukin-8; IP, immunoprecipitation; MIP-2, macrophage inflammatory protein-2; MSC, mesenchymal stem cell; oxLDL, oxidized low-density lipoprotein; p-Akt, phospho-Akt; p-eNOS, phospho-eNOS.

even with a single-dose injection. However, the effect of a single dose of MIP-2 on the aortic plaque burden was not different from that of vehicle alone (Fig. 5B). Moreover, similar to the effects of mMSCs, we also found that MIP-2 significantly increased the percentages of phospho-Akt+ and phospho-eNOS+ aortic endothelium in high-fat diet-fed apoE$^{-/-}$ mice compared with treatment with vehicle alone (Fig. 5C). These data together suggest MIP-2 is involved in mMSC-mediated effects in restoring the endothelial function.

Cell Trafficking of mMSCs

To explore whether MSCs mediate repair of atherosclerotic endothelium via engraftment, mMSCs were labeled with carboxyfluorescein succinimidyl ester (CFSE) before i.v. infusion. Aortic rings of mice infused with or without CFSE-labeled mMSCs were recovered for the detection of mMSC engraftment. We found that CFSE-labeled mMSCs could be detected at 7 days at areas close to but not actually inside the endothelium (Fig. 6), whereas few or no cells were stained with anti-CFSE Ab in those not treated with mMSCs or in control non-high-fat diet-fed wild-type mice treated with CFSE-labeled mMSCs, suggesting that a paracrine effect, rather than differentiation, contributed to the therapeutics in atherosclerosis.

The p38 Signaling Pathway Involved in the Secretion of IL8

We further elucidated the mitogen-activated protein kinase (MAPK) signaling pathway involved in the secretion of IL8 by hMSCs. First, we demonstrated that the level of phosphorylated p38 was increased in hMSCs upon exposure to oxLDL (Fig. 7A). Moreover, p38 knockdown with transient transfection of shRNA against p38 in hMSCs also inhibited IL8 expression and secretion when exposed to oxLDL (Fig. 7B, 7C). Together these data suggest that the p38/IL8 signaling pathway is involved in the mechanism of hMSC-mediated beneficial effects on endothelial dysfunction.

DISCUSSION

Endothelial dysfunction is considered the earliest change of atherosclerosis, preceding angiographic or ultrasonic evidence of atherosclerotic plaque [25]. Our study is the first to show that MSCs can be applied for treating atherosclerosis through repairing the diseased endothelium and improving endothelial function. In an animal model commonly used for atherosclerosis (apoE$^{-/-}$ mice fed a high-fat diet), mMSCs restored endothelium-dependent relaxation and decreased plaque formation. Because the lipid profile was not altered after mMSCs infusion, the beneficial effect of mMSCs does not occur through the traditional lipid-lowering effect.

The participation of chemokine in atherosclerosis has been widely studied [26]. IL8 and its receptor CXCR2, or MIP-2, play an essential role in the chemotaxis and activation of leukocytes at the early stages of atherogenesis [27, 28]. Despite its association with inflammation, the protective effects of IL8 have been described in several studies. Gimbrone et al. [29] first showed that IL8 inhibits neutrophil adhesion to cytokine-activated endothelial cells and protects these cells from neutrophil-mediated damage. IL8 directly enhances endothelial cell proliferation, survival, and matrix metalloproteinases expression and regulates angiogenesis [30]. IL8 is involved in the balance between vasoconstriction and vasodilatation and also between coagulation and fibrinolysis in

cultured endothelial cells [31]. IL8-mediated vascular endothelial growth factor receptor 2 transactivation has been reported to induce endothelial permeability [32].

In our in vitro and in vivo studies, MSCs exert their protective effect on oxLDL-treated endothelial cell through the paracrine effect by secreting IL8/MIP-2. Our in vitro study demonstrated that p38 was activated in hMSCs upon exposure to oxLDL. Moreover, we demonstrated that knockdown of p38 in hMSCs inhibited its expression and secretion of IL8 upon exposure to oxLDL. We also revealed that the PI3K inhibitor LY294002 significantly blocked the beneficial effect of hMSCs, CM-hMSC, or IL8 on ox-LDL-induced inactivation of the Akt/eNOS pathway, and the effect was similar to that of IL8 Ab. It seems that both the p38 and PI3K/Akt signaling pathways are involved in the mechanism of hMSC-mediated beneficial effects on oxLDL-treated endothelial dysfunction. However, the secretion of IL8 by MSCs via p38 activation has not been demonstrated in vivo. Because diverse signaling pathways downstream of p38 and the dual role of IL8 in its capabilities of promoting and protecting against inflammation have been observed, the interaction between different pathways and the regulation and balance among the different signaling events remained to be further studied. The generally pleiotropic effects of IL8 will demand high specificity of action and effective targeting to prevent unwanted adverse side effects [33].

There are limitations of the current study that should be noted. The effects of MSCs on the protection of endothelial cells from atherosclerosis-induced injuries have been demonstrated in both in vitro human cell cultures and in vivo mouse studies. Although the hMSCs have normal karyotypes [3], it is noteworthy that expanded mMSCs have karyotypic abnormalities with the lack of functional p53 [1, 4]. The results obtained by mMSCs should be well analyzed in detail upon application for clinical uses. Another potential limitation is the discrepancy between the therapeutic effects and the mechanisms of action of infused MSCs on endothelial dysfunction and plaque burden. Our data indicate that MIP-2 does not recapitulate the observed effects of MSCs on plaque burden in vivo and therefore the mechanism by which MSCs reduce plaque formation remains indeterminate. Further studies are required to identify other factors that MSCs mediated to reduce plaque formation in the current study. Besides, the data also indicate that changes in phospho-Akt, phospho-eNOS, and acetylcholine-induced relaxation are not reliable predictors of plaque formation in the experimental animal model. Although endothelial dysfunction has been demonstrated in most disease conditions that predict high cardiovascular risk, the association between endothelial dysfunction, different cardiovascular risk factors, and disease conditions is complex and involves an interplay with environmental conditions, local factors, and currently unknown factors [34]. Previous studies reported that the paracrine effects of MSCs play a role in the recruitment of macrophage and endothelial cell [35], inhibition of smooth muscle cell proliferation and migration [36], stimulation of neovascularization [17], and protection from ischemic injury [37], all of which are involved in different stages of atherosclerosis and plaque formation. All of these paracrine effects of MSCs may help to explain that changes in phospho-Akt, phospho-eNOS, and acetylcholine-induced relaxation are not reliable predictors of plaque formation in the current study. Further study is required to explain the discrepancies between the roles of MIP-2 in the amelioration of endothelial dysfunction and plaque formation.

Regarding the long-term effects of treatment with MSCs, we did not observe differences in endothelial dysfunction and plaque
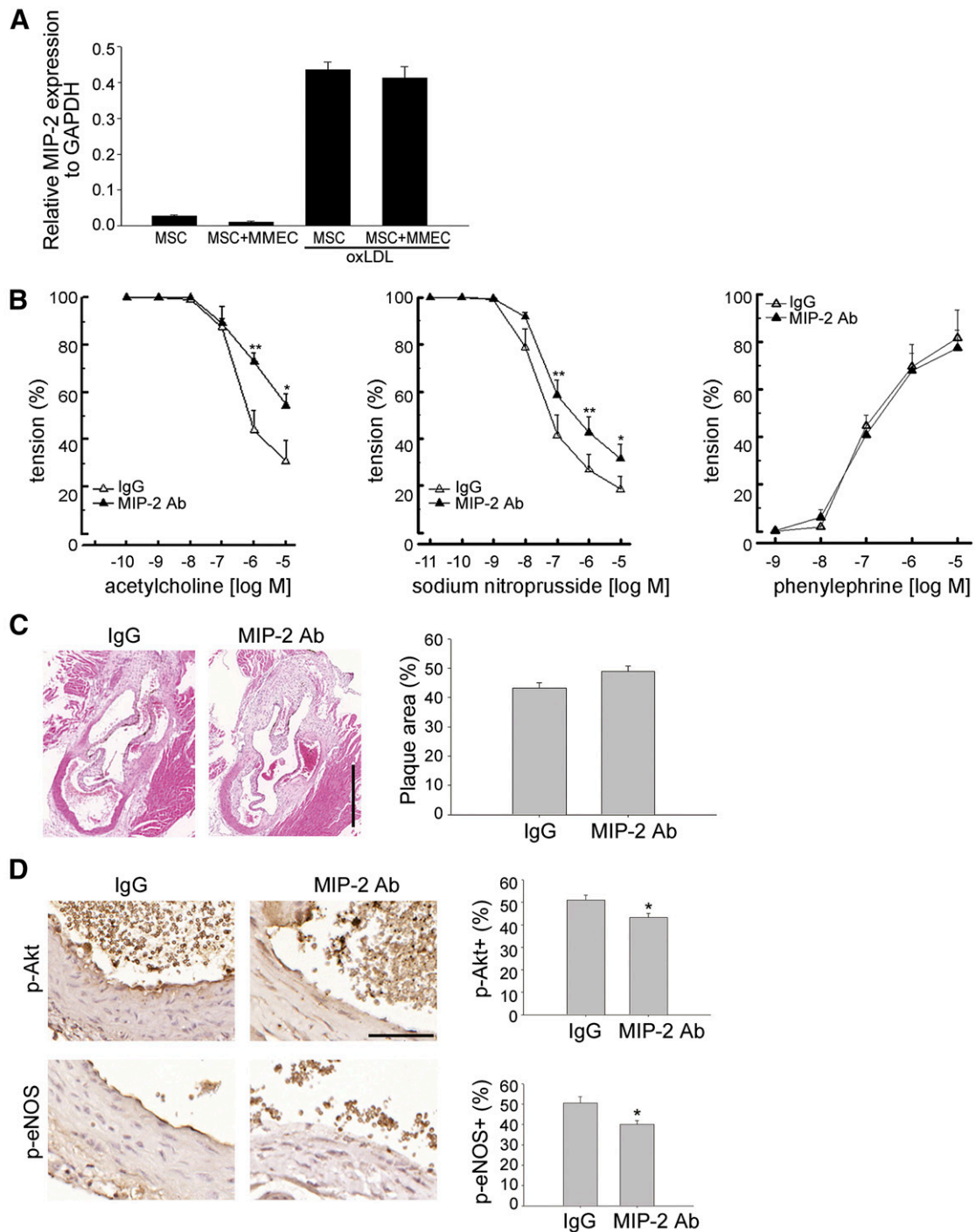
Figure 4. MSC-mediated effects on high-fat diet-fed apoE$^{-/-}$ mice depends on MIP-2. **(A):** Mouse MSCs without or with indirect coculture with MMECs in the absence or presence of 50 μg/ml oxLDL for 24 hours were assayed for quantitative RT-PCR. **(B–D):** High-fat diet-fed apoE$^{-/-}$ mice treated with MSCs (2 × 10^5 cells) that were pretreated with MIP-2 Ab or control isotype IgG were sacrificed at 1 week after treatment. The thoracic aortic rings were isolated freshly for determining the concentration-response curves **(B)** of acetylcholine-dependent relaxation (left), sodium nitroprusside-dependent relaxation (middle), and phenylephrine-dependent contraction (right) (n = 5–6 in each group). $*$, $p <$ .05; $**$, $p <$ .01 MIP-2 Ab versus control isotype IgG at the indicated concentrations. **(C):** Representative aortic root microsections show the plaque formation (left). Right: Quantitative data are expressed as percentages of immunopositive cells of total endothelial lining cells (n = 3–4 in each group). **(D):** Immunostaining of phospho-Akt and phospho-eNOS protein expression (left). Representative aortic root sections show phospho-Akt and phospho-eNOS expression in the endothelial lining. Right: Quantitative data are expressed as percentages of immuno-positive cells of total endothelial lining cells (n = 3–4 in each group). $*$, $p <$ .05. Scale bars = 500 μm **(C)**, 50 μm **(D)**. Magnification, ×40 **(C)**, ×400 **(D)**. Abbreviations: Ab, antibody; GAPDH, glyceraldehyde-3-phosphate dehydrogenase; MIP-2, macrophage inflammatory protein-2; MMEC, mouse brain microvascular endothelial cell; MSC, mesenchymal stem cell; oxLDL, oxidized low-density lipoprotein; p-Akt, phospho-Akt; p-eNOS, phosphorylated endothelial nitric-oxide synthase.
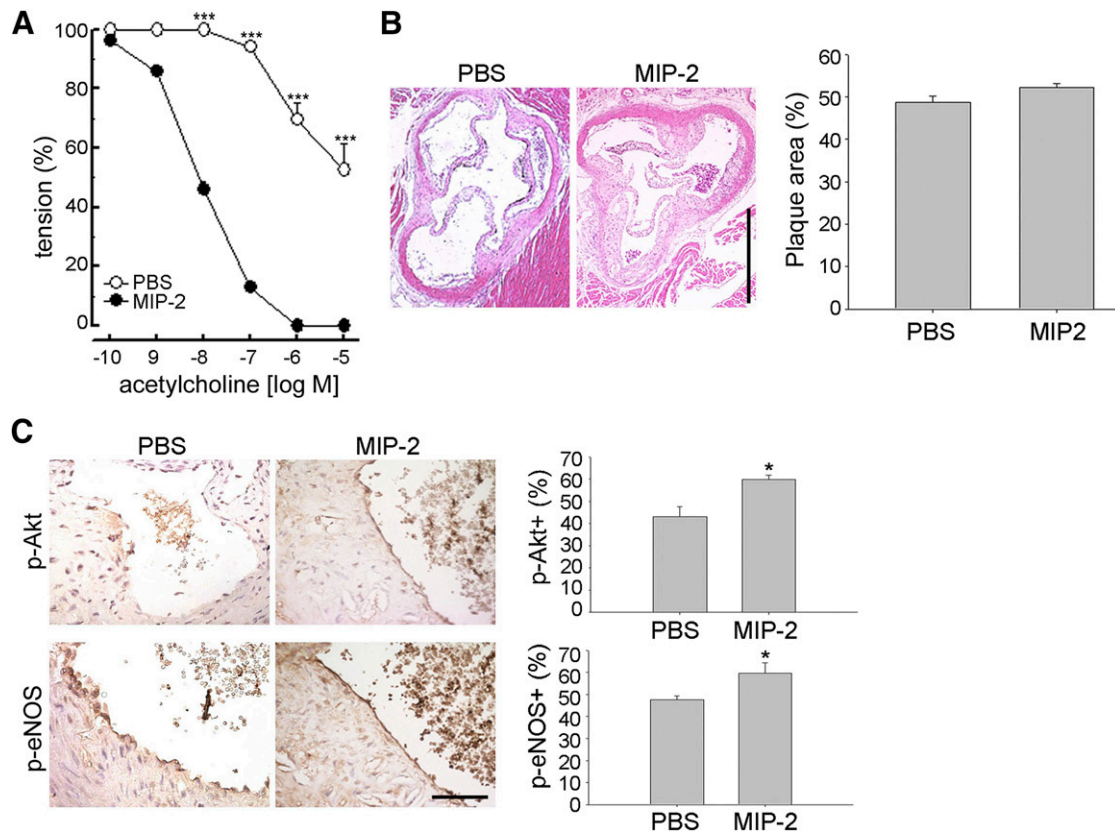
Figure 5. MIP-2 restores endothelium-dependent relaxation. High-fat diet-fed apoE$^{-/-}$ mice treated without (PBS, vehicle control) or with MIP-2 (50 μg/kg) were sacrificed at 1 week after treatment. **(A):** The thoracic aortic rings were isolated freshly for determining the concentration-response curves of acetylcholine-dependent relaxation ($n = 5$–6 in each group). ∗∗∗, $p < .001$ MIP-2 versus vehicle control at the indicated concentrations. **(B):** Representative aortic root microsections show the plaque formation (left). Right: Quantitative data are expressed as percentages of the total luminal surface area of the aorta ($n = 3$–4 in each group). **(C):** Immunostaining of phospho-Akt and phospho-eNOS protein expression (left). Representative aortic root sections show phospho-Akt and phospho-eNOS expression in the endothelial lining. Right: Quantitative data are expressed as percentages of immunopositive cells of total endothelial lining cells ($n = 3$–4 in each group). ∗, $p < .05$. Scale bars = 500 μm **(B)**, 50 μm **(C)**. Magnification, ×40 **(B)**, ×400 **(C)**. Abbreviations: MIP-2, macrophage inflammatory protein-2; p-Akt, phospho-Akt; PBS, phosphate-buffered saline; p-eNOS, phosphorylated endothelial nitric-oxide synthase.
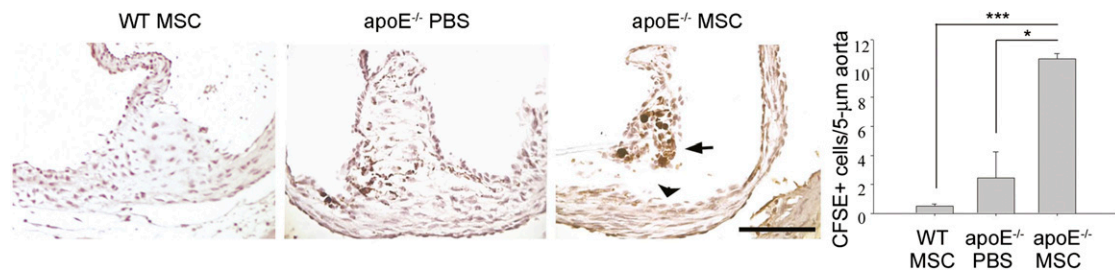

Figure 6. In vivo trafficking of transplanted mouse MSC. Non-high-fat diet-fed WT or high-fat diet-fed apoE$^{-/-}$ mice treated without (PBS, vehicle control) or with CFSE-labeled MSCs (2 × 10^5 cells) were sacrificed at 1 week after treatment, and aortic rings were recovered for immunohistochemistry study using anti-CFSE antibody. Representative pictures show CFSE-labeled MSCs (arrow) that are distant from the endothelial lining (arrowhead). ∗, $p < .05$; ∗∗∗, $p < .005$. Scale bar = 100 μm. Magnification, ×200. Abbreviations: CFSE, carboxyfluorescein succinimidyl ester; MIP-2, macrophage inflammatory protein-2; MSC, mesenchymal stem cell; PBS, phosphate-buffered saline; WT, wild type.

burden between the mice receiving intravenous infusion of MSCs and those receiving vehicle controls at 28 days after treatment (data not shown). These data suggest two possibilities. First, high-fat diet-induced endothelial dysfunction and plaque formation were reversible after a shift to normal diet as shown in our study and previous studies [38]. Thus, the endothelial dysfunction and plaque burden of mice treated with MSCs or vehicle controls

would return to normal. Second, the therapeutic effects of infused MSCs might not sustain for a long-term, which might be attributed by the removal of engrafted donor MSCs in the aorta by either a host-dependent or -independent mechanism. To maintain the therapeutic effects of intravenous infusion of MSCs on atherosclerosis-induced endothelial dysfunction and plaque formation, a secondary dose of MSC infusion is required in the future;
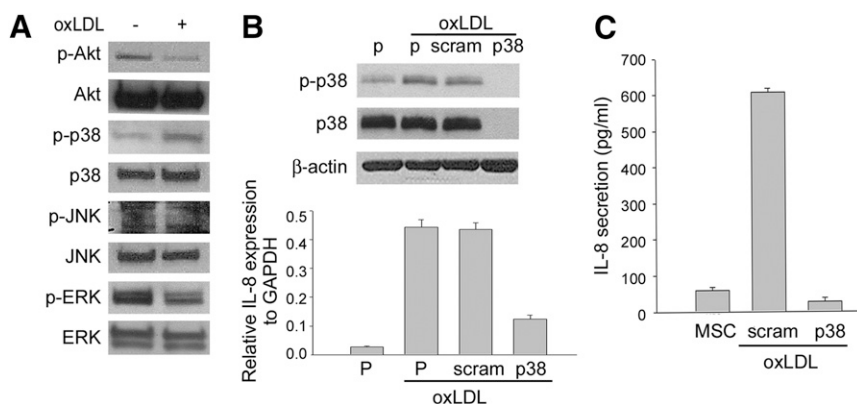
Figure 7. The expression and secretion of IL8 by MSCs depends on oxLDL-activated p38 mitogen-activated protein kinases (MAPK). **(A):** Western blot analysis for the effect of oxLDL on the activated MAPK pathways. The level of phosphorylated p38 was increased in MSCs upon exposure to 50 μg/ml oxLDL, whereas other signaling pathways were not activated. **(B, C);** p38 knockdown with transient transfection of shRNA against p38 in MSCs inhibited IL8 expression **(B)** and secretion **(C)** as assayed by Western blotting (**[B]**, upper), quantitative reverse transcription-polymerase chain reaction (**[B]**, lower), and enzyme-linked immunosorbent assay **(C)**. Abbreviations: ERK, extracellular signal-regulated kinase; GAPDH, glyceraldehyde-3-phosphate dehydrogenase; IL-8, interleukin-8; JNK, c-Jun N-terminal kinase; MSC, mesenchymal stem cell; oxLDL, oxidized low-density lipoprotein; P, parental; p38, p38-specific shRNA; p-Akt, phospho-Akt; p-ERK, phospho-ERK; p-JNK, phospho-JNK; p-p38, phospho-p38; scram, scrambled shRNA.

the results of the current preliminary study would be helpful in the development of protocols for future preclinical or clinical trials in the application of MSCs for atherosclerosis treatment.

CONCLUSION

This study was aimed to identify the effect of MSCs in the early stage of atherosclerosis for earlier prevention of the development and/or progression of disease. However, further studies need to identify measures to maintain the beneficial effect of MSCs for a long time and to understand more about the complex mechanism underlying the MSCs transplantation in different stages of atherosclerosis. Nevertheless, the current data suggest that MSCs promote endothelial function through releasing a repertoire of paracrine factors via activation of p38 MAPK, and the MSCs or their secretome may be applied to treat atherosclerosis in patients.

AUTHOR CONTRIBUTIONS

Y.-L.L.: conception and design, collection and/or assembly of data, data analysis and interpretation, manuscript writing, final approval of manuscript; S.-F.Y.: provision of transgenic animal and experimental protocols; Y.-T.H.: collection and/or assembly of data, data analysis and interpretation; G.-J.W. and S.-C.H.: conception and design, data analysis and interpretation, manuscript writing, final approval of manuscript.

DISCLOSURE OF POTENTIAL CONFLICTS OF INTEREST

The authors indicate no potential conflicts of interest.

REFERENCES

1 Hansson GK. Inflammation, atherosclerosis, and coronary artery disease. N Engl J Med 2005;352:1685–1695.

2 Witztum JL, Steinberg D. Role of oxidized low density lipoprotein in atherogenesis. J Clin Invest 1991;88:1785–1792.

3 Morawietz H, Duerrschmidt N, Niemann B et al. Induction of the oxLDL receptor LOX-1 by endothelin-1 in human endothelial cells. Biochem Biophys Res Commun 2001;284:961–965.

4 Li D, Mehta JL. Antisense to LOX-1 inhibits oxidized LDL-mediated upregulation of monocyte chemoattractant protein-1 and monocyte adhesion to human coronary artery endothelial cells. Circulation 2000;101:2889–2895.

5 Blair A, Shaul PW, Yuhanna IS et al. Oxidized low density lipoprotein displaces endothelial nitric-oxide synthase (eNOS) from plasmalemmal caveolae and impairs eNOS activation. J Biol Chem 1999;274:32512–32519.

6 Vieira O, Escargueil-Blanc I, Jurgens G et al. Oxidized LDLs alter the activity of the ubiquitin-proteasome pathway: Potential role in oxidized LDL-induced apoptosis. FASEB J 2000;14:532–542.

7 Vallance P, Benjamin N, Collier J. The effect of endothelium-derived nitric oxide on ex vivo whole blood platelet aggregation in man. Eur J Clin Pharmacol 1992;42:37–41.

8 Félétou M. The Endothelium: Part 1: Multiple Functions of the Endothelial Cells—Focus on Endothelium-Derived Vasoactive Mediators. San Rafael, CA: Morgan & Claypool Life Sciences, 2011.

9 Fulton D, Gratton JP, McCabe TJ et al. Regulation of endothelium-derived nitric oxide production by the protein kinase Akt. Nature 1999; 399:597–601.

10 Chavakis E, Dernbach E, Hermann C et al. Oxidized LDL inhibits vascular endothelial growth factor-induced endothelial cell migration by an inhibitory effect on the Akt/endothelial nitric oxide synthase pathway. Circulation 2001;103:2102–2107.

11 Stangl K, Stangl V. The ubiquitin-proteasome pathway and endothelial (dys) function. Cardiovasc Res 2010;85:281–290.

12 Prockop DJ. Marrow stromal cells as stem cells for nonhematopoietic tissues. Science 1997;276:71–74.

13 Nagaya N, Fujii T, Iwase T et al. Intravenous administration of mesenchymal stem cells

improves cardiac function in rats with acute myocardial infarction through angiogenesis and myogenesis. Am J Physiol Heart Circ Physiol 2004;287:H2670–H2676.

14   Huang WH, Chen HL, Huang PH et al. Hypoxic mesenchymal stem cells engraft and ameliorate limb ischaemia in allogeneic recipients. Cardiovasc Res 2014;101:266–276.

15   Madonna R, Taylor DA, Geng YJ et al. Transplantation of mesenchymal cells rejuvenated by the overexpression of telomerase and myocardin promotes revascularization and tissue repair in a murine model of hindlimb ischemia. Circ Res 2013;113:902–914.

16   Gnecchi M, He H, Liang OD et al. Paracrine action accounts for marked protection of ischemic heart by Akt-modified mesenchymal stem cells. Nat Med 2005;11:367–368.

17   Kinnaird T, Stabile E, Burnett MS et al. Local delivery of marrow-derived stromal cells augments collateral perfusion through paracrine mechanisms. Circulation 2004;109:1543–1549.

18   Fraga CG, Leibovitz BE, Tappel AL. Lipid peroxidation measured as thiobarbituric acid-reactive substances in tissue slices: Characterization and comparison with homogenates and microsomes. Free Radic Biol Med 1988;4:155–161.

19   Lowry OH, Rosebrough NJ, Farr AL et al. Protein measurement with the Folin phenol reagent. J Biol Chem 1951;193:265–275.

20   Tsai CC, Chen YJ, Yew TL et al. Hypoxia inhibits senescence and maintains mesenchymal stem cell properties through down-regulation of E2A-p21 by HIF-TWIST. Blood 2011;117:459–469.

21   Yew TL, Chang MC, Hsu YT et al. Efficient expansion of mesenchymal stem cells from mouse bone marrow under hypoxic conditions. J Tissue Eng Regen Med 2013;7:984–993.

22   Coisne C, Dehouck L, Faveeuw C et al. Mouse syngenic in vitro blood-brain barrier model: A new tool to examine inflammatory events in cerebral endothelium. Lab Invest 2005;85:734–746.

23   Wang GJ, Shan J, Pang PK et al. The vasorelaxing action of rutaecarpine: Direct paradoxical effects on intracellular calcium concentration of vascular smooth muscle and endothelial cells. J Pharmacol Exp Ther 1996; 276:1016–1021.

24   Karp JM, Leng Teo GS. Mesenchymal stem cell homing: The devil is in the details. Cell Stem Cell 2009;4:206–216.

25   Lüscher TF, Barton M. Biology of the endothelium. Clin Cardiol 1997;20(suppl 2): II-3–II-10.

26   Terkeltaub R, Boisvert WA, Curtiss LK. Chemokines and atherosclerosis. Curr Opin Lipidol 1998;9:397–405.

27   Hechtman DH, Cybulsky MI, Fuchs HJ et al. Intravascular IL-8. Inhibitor of polymorphonuclear leukocyte accumulation at sites of acute inflammation. J Immunol 1991;147: 883–892.

28   Schmal H, Shanley TP, Jones ML et al. Role for macrophage inflammatory protein-2 in lipopolysaccharide-induced lung injury in rats. J Immunol 1996;156:1963–1972.

29   Gimbrone MA Jr., Obin MS, Brock AF et al. Endothelial interleukin-8: A novel inhibitor of leukocyte-endothelial interactions. Science 1989;246:1601–1603.

30   Li A, Dubey S, Varney ML et al. IL-8 directly enhanced endothelial cell survival, proliferation, and matrix metalloproteinases production and regulated angiogenesis. J Immunol 2003;170:3369–3376.

31   Cheng M, Li Y, Wu J et al. IL-8 induces imbalances between nitric oxide and endothelin-1, and also between plasminogen activator inhibitor-1 and tissue-type plasminogen activator in cultured endothelial cells. Cytokine 2008;41:9–15.

32   Petreaca ML, Yao M, Liu Y et al. Transactivation of vascular endothelial growth factor receptor-2 by interleukin-8 (IL-8/CXCL8) is required for IL-8/CXCL8-induced endothelial permeability. Mol Biol Cell 2007;18:5014–5023.

33   Kleemann R, Zadelaar S, Kooistra T. Cytokines and atherosclerosis: A comprehensive review of studies in mice. Cardiovasc Res 2008;79: 360–376.

34   Reriani MK, Lerman LO, Lerman A. Endothelial function as a functional expression of cardiovascular risk factors. Biomarkers Med 2010;4:351–360.

35   Chen L, Tredget EE, Wu PY et al. Paracrine factors of mesenchymal stem cells recruit macrophages and endothelial lineage cells and enhance wound healing. PLoS One 2008;3:e1886.

36   Wu X, Huang L, Zhou Q et al. Mesenchymal stem cells participating in ex vivo endothelium repair and its effect on vascular smooth muscle cells growth. Int J Cardiol 2005;105: 274–282.

37   Jiang S, Haider HK, Idris NM et al. Supportive interaction between cell survival signaling and angiocompetent factors enhances donor cell survival and promotes angiomyogenesis for cardiac repair. Circ Res 2006;99: 776–784.

38   Wassmann S, Werner N, Czech T et al. Improvement of endothelial function by systemic transfusion of vascular progenitor cells. Circ Res 2006;99:e74–e83.

See www.StemCellsTM.com for supporting information available online.